ELSEVIER

Journal of Alloys and Compounds 317–318 (2001) 115–119

Journal of ALLOYS AND COMPOUNDS

www.elsevier.com/locate/jallcom

Structure, magnetism and electrical conductivity of a new ternary manganese oxide: $BaMn_3O_6$

Koji Wakiya[a], Hirohiko Sato[a,*], Akira Miyazaki[a], Toshiaki Enoki[a], Masahiko Isobe[b], Yutaka Ueda[b]

[a]*Department of Chemistry, Tokyo Institute of Technology, 2-12-1 Ookayama, Meguro-ku, Tokyo 152-8551, Japan*
[b]*Institute for Solid State Physics, University of Tokyo, 7-22-1 Roppongi, Minato-ku, Tokyo 106-8666, Japan*

Abstract

The structure, magnetic susceptibility and conductivity of a newly synthesized manganese oxide ($BaMn_3O_6$) are reported. Single crystal structure analysis revealed a layered structure. Two types of layers, (I) double layers composed of edge-shared MnO_6 octahedra and (II) perovskite-like layers composed of vertex-shared MnO_6, are stacked alternatively. All MnO_6 octahedra are strongly distorted due to the Jahn–Teller effect. Although the chemical formula $BaMn_3O_6$ indicates a mixed-valence state of Mn^{3+} and Mn^{4+}, the electrical conductivity shows an activation-type temperature dependence, suggesting a semiconductive band structure or Mott-type insulating electronic states. Magnetic susceptibility measurement revealed an antiferromagnetic transition at $T_N = 295$ K. Above T_N, the magnetic susceptibility exhibits almost temperature-independent behavior. This deviation from molecular-field behavior can be attributed to a large frustration effect originating from the topology of the magnetic-interaction network.

Keywords: Manganese oxides; Mixed-valence; Mott insulator; Antiferromagnetism; Frustration; Semiconductor; Jahn–Teller effect

1. Introduction

Recently, manganese oxides have aroused the interest of chemists for their variety of crystal structures [1], and also of physicists for their novel physical properties such as the colossal magnetoresistance (CMR) [2]. Manganese oxides with a mixed-valence state, especially systems where Mn^{3+} and Mn^{4+} coexist, are very attractive materials because we expect electrical conduction and magnetism. Generally, in manganese oxides, the d electrons are in a high-spin state and the electronic configurations for Mn^{3+} and Mn^{4+} are expressed as $t_{2g}^3e_g$ ($S = 2$) and t_{2g}^3 ($S = 3/2$), respectively, where S indicates the spin for each configuration. Therefore, the electronic conduction in Mn^{3+}–Mn^{4+} mixed-valence compounds is anomalous because itinerant electrons from band-like e_g orbitals are strongly coupled with localized electrons in t_{2g} orbitals via Hund's rule. This causes an interesting phenomenon, ferromagnetism, induced by a double exchange interaction, CMR, the spin polaron effect, etc.

From a structural point of view, Mn^{3+}–Mn^{4+} mixed-valence oxides based on the MnO_6 octahedron are roughly classified into vertex-shared type compounds such as perovskite and edge-shared type compounds such as rutile or hollandite. Most physical studies have concentrated on the former series because the 'orbital' degree of freedom plays an important role [3] in addition to charge, spin and lattice degrees of freedom. On the other hand, very little is known about the physical properties of edge-shared type manganese oxides. Recently, we revealed interesting electronic and magnetic phase transitions in hollandite type manganese oxides [4,5] and strong coupling between electric conduction and magnetism in rutile type manganese oxide [6]. As a next step, we performed a search for new materials with the Mn^{3+}–Mn^{4+} mixed-valence state and discovered of a new phase, $BaMn_3O_6$. In this paper, we report its novel structure as a hybrid of an edge-shared network and a vertex-shared network of MnO_6 octahedra, and its interesting physical properties including a high temperature antiferromagnetic transition with a large frustration.

2. Experimental

Single crystals of $BaMn_3O_6$ were synthesized by a hydrothermal method using a test-tube type autoclave. Ten milligrams of aktenskite (ε-MnO_2) powder and 50 mg of $Ba(OH)_2$ were sealed with 0.3 ml of water in a silver capsule (5 mm $\phi \times 70$ mm). After reaction under 150 MPa

*Corresponding author.

0925-8388/01/$ – see front matter
PII: S0925-8388(00)01320-7

at 525°C for 48 h, the capsule was quenched at room temperature. Many black, rectangular-parallelepiped crystals formed in the capsule. Their typical size was $0.3\times 0.1\times 0.05$ mm^3. EPMA analysis on a crystal revealed that the atomic ratio of Ba to Mn is almost 1:3.

For the determination of the crystal structure, a black plate-like crystal was mounted on a Rigaku AFC-7R four-circle diffractometer. Six hundred and sixty-four reflections ($7.5<2\theta<55°$) were collected with ω–2θ scan using Mo Kα radiation, and 616 independent reflections ($|F_o|>4\sigma(|F_o|)$) were used for further analysis. The absorption effect was corrected using an empirical ψ-scan method. The crystal structure was solved by direct methods (SHELXS86) and refined by a full-matrix least-squares method on F^2 (SHELXL93). As shown below, the chemical formula was found to be $BaMn_3O_6$ from the result of EPMA and structural analysis.

The magnetic susceptibility was measured using a SQUID magnetometer (Quantum Design MPMS-5) on a non-oriented polycrystalline sample for determination of the absolute value and measured on a single crystal for the study of anisotropy. The applied magnetic field was 1 T and the temperature range was between 2 and 700 K. In the case of measurement at high temperature, the sample was sealed in a quartz capsule with oxygen gas in order to avoid decomposition. Electrical conductivities were measured by the dc four-terminal method. Gold wires were attached to a single crystal with carbon paste. Ohmic I–V characteristics were confirmed before the measurements.

3. Results and discussion

3.1. Crystal structure

Table 1 summarizes the crystal data and the final reliable factors. The final atomic parameters are summarized in Table 2. A schematic view of the structure projected to the *ac* plane and to the *ab* plane is shown in Figs. 1 and 2, respectively. As seen clearly from the figures, $BaMn_3O_6$ exhibits a layered structure. There are two types of layers: double layers composed of an edge-

Table 1
Summary of crystal data and refinement results

Structural formula	$BaMn_3O_6$
Formula weight	398.14
Crystal size (mm^3)	$0.167\times 0.117\times 0.067$
a (Å)	19.537(1)
b (Å)	4.529(1)
c (Å)	5.583(1)
β (deg)	98.19(1)
V (Å^3)	489.0(2)
Z	4
Space group	$C2/m$
ρ_{calc} (g/cm^3)	5.409
$R(F)$	4.48%

Table 2
Fractional atomic coordinates and equivalent isotropic displacement parameters (Å^2) with esd's in parentheses

Atom	x	y	z	U_{eq}
Ba1	0.07480(2)	0.0	0.28763(6)	0.0084(2)
Mn1	0.20903(6)	0.5	0.3552(2)	0.0048(3)
Mn2	0.21123(6)	0.5	0.8551(2)	0.0056(3)
Mn3	0.06470(7)	0.5	0.7824(2)	0.0051(3)
O1	0.2778(3)	0.5	0.6351(9)	0.008(1)
O2	0.2764(3)	0.5	0.142(1)	0.007(1)
O3	0.0726(3)	0.0	0.7857(9)	0.007(1)
O4	0.1412(3)	0.5	0.062(1)	0.010(1)
O5	0.1411(3)	0.5	0.580(1)	0.009(1)
O6	0.0	0.5	0.5	0.008(1)
O7	0.0	0.5	0.0	0.008(1)

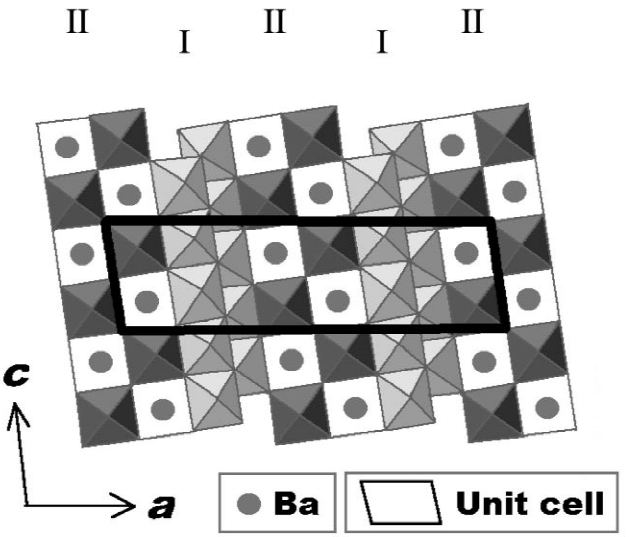

Fig. 1. Schematic view of the crystal structure of $BaMn_3O_6$ projected to the *ac* plane.

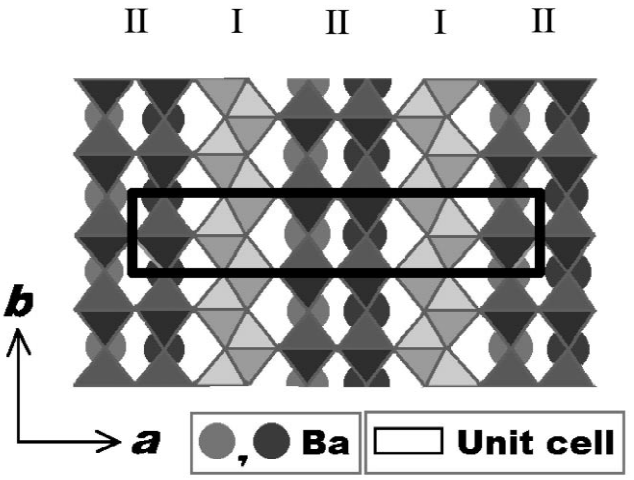

Fig. 2. Schematic view of the crystal structure of $BaMn_3O_6$ projected to the *ab* plane.

shared network of MnO_6 octahedra (layer I), and layers including vertex-shared octahedra and Ba ions (layer II). We see the layer I structure commonly in β-$NaMnO_2$ [7]. On the other hand, the layer II structure is locally equivalent to the perovskite structure. Therefore, we can conclude that $BaMn_3O_6$ has a unique crystal structure that can be interpreted as a hybrid of edge-shared type manganese oxides and perovskite. There are three crystallographic sites for Mn, as shown in the scheme in Table 3. Site A is located in layer II, while both B and C are within layer I. Site B differs from site C for the edge-shared contact with site A.

From Table 3 it is clear that all of the MnO_6 octahedra are strongly distorted. The most probable origin of this distortion is the Jahn–Teller effect due to the presence of Mn^{3+} with the d^4 electronic configuration. Based on the ionic picture, $BaMn_3O_6$ is formally described as $Ba^{2+}Mn_2^{3+}Mn^{4+}O_6^{2-}$. This tempts us to place two Mn^{3+} ions and one Mn^{4+} at three crystallographically independent manganese sites. However, it is not straightforward to determine the Mn^{3+} and Mn^{4+} sites from crystal data only. One possible way at present is to place Mn^{4+} at the perovskite-like sites (site A) because the average Mn–O distance around them is the shortest, although the magnitude of the Jahn–Teller-like distortions is not so different for each site.

3.2. Magnetic susceptibility

Fig. 3 shows the temperature dependence of the magnetic susceptibility. A magnetic phase transition was found at $T_N = 295$ K. Below T_N, the magnetic susceptibility in the magnetic field along the *b*-axis goes to zero as the temperature approaches zero, while the susceptibility along the other two axes remains almost constant. This shows that the easy spin axis of the antiferromagnetic phase is the *b*-axis. Because $BaMn_3O_6$ is considered to be a mixed-spin system of $S = 2$ (for Mn^{3+}) and $S = 3/2$ (for Mn^{4+}), we can expect a ferrimagnetic phase. However, the magnetization curve does not show spontaneous magnetization but exhibits an almost straight line for the magnetic field along any direction up to the limit of our instrument, 5.5 T. We can also exclude the possibility of helical magnetism, which appears in several manganese oxides such as β-MnO_2 [8], because the susceptibility along the *b*-axis goes to zero at $T = 0$ K.

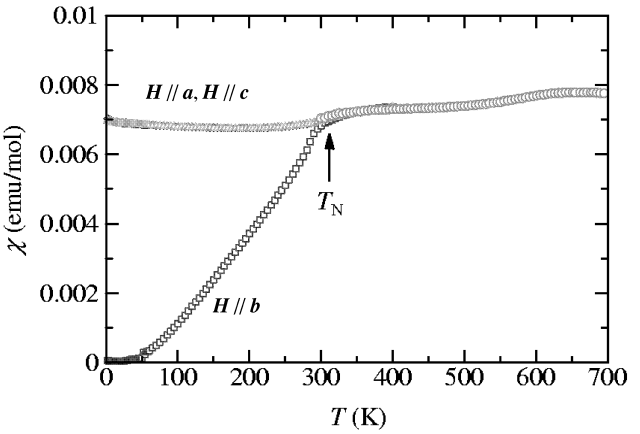

Fig. 3. Temperature dependence of the magnetic susceptibility of $BaMn_3O_6$. The curve for $H//a$ and for $H//c$ below T_N is almost the same.

The magnetic susceptibility above T_N is weakly temperature dependent. It gradually increases with increasing temperature showing a broad maximum around 650 K. Since the cooling curve completely agrees with the warming curve, we consider that the maximum around 650 K is an intrinsic effect. It is obvious that molecular field analysis above T_N is not appropriate because of the absence of Curie–Weiss type behavior. This large deviation of the behavior above T_N from molecular field theory qualitatively resembles what is observed in low-dimensional antiferromagnets. For example, the one-dimensional antiferromagnet $CsMnCl_3 \cdot 2H_2O$ or the two-dimensional antiferromagnet K_2NiF_4 show a broad maximum in magnetic susceptibility far above T_N [9,10]. However, the crystal structure of $BaMn_3O_6$ suggests a three-dimensional network of an exchange interaction. Why does this compound behave like a low-dimensional magnet?

As shown below, it is noted that a topological frustration is inherent within the double-layered structure of the edge-shared MnO_6 octahedra (layer I). Fig. 4 shows the structure of layer I seen from the *a*-axis, emphasizing the Mn sites with circles. Since the network of exchange interactions forms a quasi-triangular lattice, it is obvious that there is no net exchange interaction between the 'upper' chains and the 'lower' chains within a molecular-field approximation for two-sublattice antiferromagnetism.

Table 3
Detailed information about the Mn–O bonds of the MnO_6 octahedron. A, B, and C denote the three crystallographically independent sites of Mn atoms. Numbers (1)–(6) denote oxygen atoms

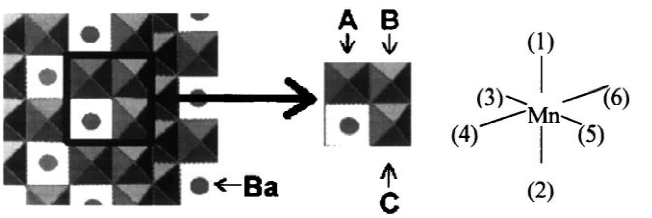

	Site A	Site B	Site C
(1)–Mn–(2) (deg)	172.3	167.9	167.1
(1)–Mn (Å)	2.27	2.28	2.28
(2)–Mn (Å)	2.27	2.28	2.28
(3)–Mn (Å)	2.00	1.90	1.91
(4)–Mn (Å)	2.00	1.92	1.89
(5)–Mn (Å)	1.88	1.91	1.95
(6)–Mn (Å)	1.88	1.91	1.95

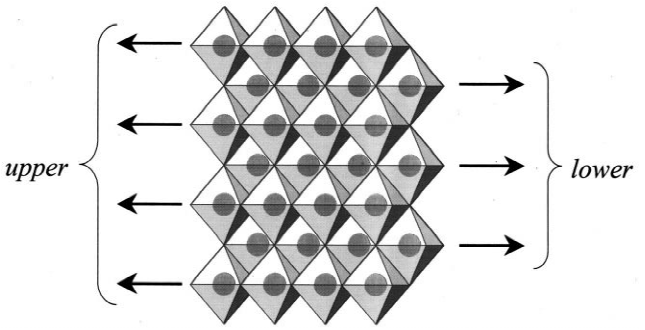

Fig. 4. Schematic view of layer I seen from the *a*-axis. Each circle indicates Mn ions located at the center of the MnO_6 octahedron. It is clear that Mn ions form a quasi-triangular network of an exchange interaction.

This should effectively prevent three-dimensional magnetic ordering. We believe that this is why $BaMn_3O_6$ behaves like a low-dimensional antiferromagnet. Strictly speaking, the B and C sites are not equivalent, but their local circumstances are very similar. Therefore, we expect a large frustration, although it is not perfect.

3.3. Conductivity

We measured the electrical conductivity in expectation of a metallic electronic state. However, it shows an activation-type temperature dependence as shown in Fig. 5. The conductivity and the activation energy at 300 K for the case of $\boldsymbol{I}//\boldsymbol{c}$ are about 10^{-4} S cm^{-1} and 0.54 eV, respectively, while those for $\boldsymbol{I}//\boldsymbol{b}$ are 10^{-5} S cm^{-1} and 0.40 eV. Because of the shape of the crystal, we have not been successful with measurement with the current along the *a*-axis. There are two possible explanations for the non-metallic electronic state. Firstly, we cannot exclude the possibility that $BaMn_3O_6$ is a band insulator because there are an even number of d electrons in a unit cell. Another possibility is that it is a Mott insulator because of the strong on-site Coulomb repulsion between the e_g electrons. We cannot conclude which is correct at present, but the observed anisotropy in activation energy needs a model based on a hopping-conduction mechanism beyond a simple band-semiconductor picture.

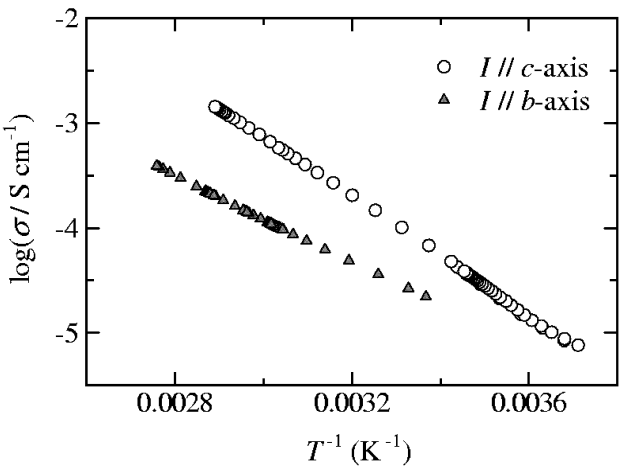

Fig. 5. Temperature dependence of the electrical conductivity of $BaMn_3O_6$. *I* is the electric current.

Robin and Day classified mixed-valence compounds by the strength of the charge-transfer interaction between the metal ions in different valence states [11]. If we place Mn^{3+} ions at sites B and C, and Mn^{4+} ions at site A, the charge-transfer interaction between Mn^{3+} and Mn^{4+} should be very weak because of the large difference in the coordination circumstances. In that case, $BaMn_3O_6$ is classified as a class I type mixed-valence compound [11] and, consequently, we cannot expect a large conductivity along the a^*-axis. Besides, conduction in the *bc* plane is also poor because of the absence of e_g electrons (for layer II) and a Mott-insulator like state (for layer I). Preliminary measurement of the optical reflectance spectra did not indicate any charge-transfer band in the case of polarization $\boldsymbol{E}//\boldsymbol{c}$ and $\boldsymbol{E}//\boldsymbol{b}$ [12]. This does not conflict with the above picture that the charge separation occurs along the *a*-axis. Measurement of the conductivity along the *a*-axis and measurement of the optical spectra with $\boldsymbol{E}//\boldsymbol{a}$ will provide useful information about the spatial distribution of Mn^{3+} and Mn^{4+}, although such measurements are difficult at present because of the very small size of the crystals.

One of our motivations for the conductivity measurement was to observe a strong coupling between electric conduction and magnetism. However, no anomaly was observed in the conductivity at T_N. This suggests that the activation-type conduction of the e_g electrons in $BaMn_3O_6$ is not governed by the interaction with localized magnetic moments but is mainly governed by the band-gap or Hubbard-gap, which has nothing to do directly with the magnetic order.

4. Conclusion

During a search for new materials possessing an interesting interplay between electric conduction and magnetism, we found a new phase of ternary manganese oxides, $BaMn_3O_6$. Its chemical composition indicates a mixed-valence system with Mn^{3+} and Mn^{4+}. An X-ray diffraction study revealed a unique structure based on MnO_6 octahedral units, that is an alternating stacking of edge-shared type layers and perovskite-like layers. The magnetic susceptibility revealed an antiferromagnetic transition at $T_N = 295$ K and a strong frustration effect caused by the special crystal structure including a distorted-triangular network of paths of exchange interactions. The conductivity showing activation type behavior suggests a semiconductive band structure or a Mott-insulating state. There is no large anomaly in the conductivity at T_N. For further understanding of the physical properties of this compound, a neutron diffraction study is desired in order

to clarify the charge distribution and the magnetic structure.

Acknowledgements

The authors would like to thank R. Ohki for help with the EPMA. This work was partly supported by a Grant-in-Aid for Scientific Research, Nos. 10740318 and 10149101, from the Ministry of Education, Science, Sports and Culture, Japanese Government.

References

[1] Q. Feng, H. Kanoh, K. Ooi, J. Mater. Chem. 9 (1999) 319.
[2] Y. Tokura (Ed.), Colossal Magnetoresistive Oxides, Gordon and Breach, London, 1999.
[3] Y. Murakami, H. Kawada, H. Kawata, M. Tanaka, T. Arima, Y. Moritomo, Y. Tokura, Phys. Rev. Lett. 80 (1998) 1932.
[4] H. Sato, J.-I. Yamaura, T. Enoki, N. Yamamoto, J. Alloys Comp. 262/263 (1997) 443.
[5] H. Sato, J.-I. Yamaura, T. Enoki, N. Yamamoto, Phys. Rev. B 59 (1999) 12836.
[6] H. Sato, T. Enoki, M. Isobe, Y. Ueda, Phys. Rev. B 61 (2000) 3563.
[7] J.-P. Parent, R. Olazcuaga, M. Devalette, C. Fouassier, P. Hagenmuller, J. Solid State Chem. 3 (1971) 1.
[8] A. Yoshimori, J. Phys. Soc. Jpn. 14 (1959) 807.
[9] T. Smith, S.A. Friedberg, Phys. Rev. 176 (1968) 660.
[10] K.G. Srivastava, Phys. Lett. 4 (1963) 55.
[11] M.B. Robin, P. Day, Adv. Inorg. Chem. Radiochem. 10 (1967) 247.
[12] K. Wakiya, H. Sato, T. Enoki, H. Kitagawa, T. Mitani, unpublished results.